

# Melt Rheological Properties of Polypropylene–Wood Flour Composites

S. N. MAITI and M. R. HASSAN, *Centre for Materials Science and Technology, Indian Institute of Technology, Delhi, New Delhi-110016, India*

## Synopsis

This article presents study of melt rheological properties of composites of polypropylene (*i*-PP) filled with wood flour (WF), at filler concentrations of 3–20 wt%. Results illustrate the effects of (i) filler concentration and (ii) shear stress or shear rates on melt viscosity and melt elasticity properties of the composites. Incorporation of WF into *i*-PP results in an increase of its melt viscosity and a decrease of melt elasticity such as die swell and first normal stress differences; these properties, however, depend on filler concentration. Processing temperature of the filled *i*-PP increases as compared to the nonfilled polymer.

## INTRODUCTION

Isotactic polypropylene (*i*-PP) is a very useful commercial polymer containing little or no unsaturation. Its outstanding properties include: lowest density among commercial thermoplastics, exceptional flex life, good surface hardness and scratch resistance, very good abrasion resistance, high chemical resistance, excellent stress–crack resistance, steam sterilizability, and excellent electrical properties.<sup>1</sup> The scope of application of *i*-PP has been widened by making blends with other polymers such as ethylene propylene rubber,<sup>2,3</sup> styrene butadiene rubber,<sup>4</sup> acrylonitrile butadiene styrene terpolymer,<sup>5</sup> and triblock copolymer styrene–ethylene butylene–styrene,<sup>6</sup> etc. Use of various reinforcing agents such as glass fibers and asbestos with *i*-PP is also well established to suit a wide range of end uses.<sup>7–9</sup>

Use of fillers in *i*-PP for improvement of properties as well as reduction in cost is illustrated in the literature.<sup>10–13</sup> Some of the commonly used fillers for *i*-PP are talc, kaolin, calcium carbonate, carbon black, etc.

Wood flour is an inexpensive filler which reduces the cost of the polymer compound without significant loss in other strength properties. Its use in thermoset and in thermoplastic compositions<sup>14–17</sup> is well known. Decreased shrinkage after molding, increase in modulus of elasticity, and creep resistance with increasing wood flour content was reported by Ishihara et al.<sup>17</sup> in the study of *i*-PP/wood flour composites. Good mechanical properties were obtained by treating the surface of wood flour with a sizing agent.<sup>18</sup> Use of wood flour filler in various other thermoplastic compositions such as polyethylene,<sup>19</sup> polystyrene,<sup>20</sup> poly(vinyl chloride),<sup>21</sup> and nylon 66<sup>22</sup> are also reported.

In the present paper we report the study on the melt rheological properties of *i*-PP/wood flour composites. A piston type capillary rheometer was used to

obtain shear stress–shear rate data, melt viscosity, and melt elasticity parameters at various filler loadings and at various temperatures.

### EXPERIMENTAL

**Materials.** *i*-PP used was Koylene M3030 (M.F.I. 3 and density 0.89 g cm<sup>-3</sup>) supplied by Indian Petrochemicals Corporation Ltd., India. Wood flour (WF) from Deodar wood (Botanical name *Cedrus Deodara*, also known as Indian Cedar) was sieved, and the particles of size 200–300 μm (density 1.326 g cm<sup>-3</sup>) were used for the study.

**Compounding.** Wood flour was dried at 373 K for 2 h followed by vacuum drying at 333 K for 1 h to expel moisture. The dried wood flour and *i*-PP granules were fed to a plasticating Betol extruder, Model BM-1820, England, to prepare composites containing 3, 10, and 20 wt% WF. The strands coming out of the die were granulated. These granules were used in the rheometer.

**Measurements.** Melt flow properties of the *i*-PP/wood flour composites were measured on an Instron Capillary Rheometer, Model M.C.R. 1112, using a capillary die of  $L/R = 67.20$  and applied wall shear stress range 40–250 kPa at temperatures of 483, 503, and 523 K.

### RESULTS AND DISCUSSION

**Shear Stress–Shear Rate Curves.** Shear stress at the wall  $\tau_w$  of the capillary viscometer was calculated using the following formula<sup>23</sup>:

$$\tau_w = \frac{F}{4A_p(L/D)} \quad (1)$$

where  $F$  = weight force (kg),  $A_p$  = area of the plunger, and  $L$  and  $D$  are the length and diameter of the capillary.

The apparent shear rate  $\gamma_a$  was calculated using the following equation<sup>23</sup>:

$$\gamma_a = \frac{2}{15} \frac{V_{\text{ch}} d_p^2}{D^3} \quad (2)$$

where  $V_{\text{ch}}$  = crosshead speed and  $d_p$  = diameter of the plunger. From the apparent shear rate values the shear rate at the wall  $\gamma_w$  of the capillary was calculated after applying Rabinowitsch correction<sup>24,25</sup>:

$$\gamma_w = \{(3n' + 1)/4n'\} \gamma_a \quad (3)$$

where  $n'$  = flow behavior index obtained as the slope of the linear plot of  $\log \tau_w$  vs.  $\log \gamma_a$  (curves not shown).

The melt viscosity  $\eta$  was evaluated as

$$\eta = \tau_w / \gamma_w \quad (4)$$

The dependence of  $\log \gamma_w$  vs.  $\log \gamma_w'$  for the *i*-PP/WF composites were linear in the range of shear rates studied. This indicates that power law

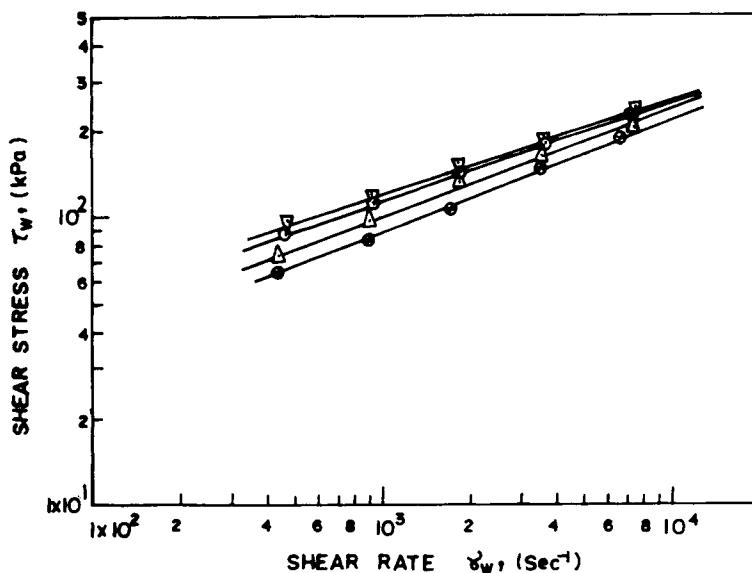


Fig. 1. Shear stress ( $\tau_w$ ) vs. shear rate ( $\gamma_w$ ) curves at 483 K: ( $\odot$ ) *i*-PP; ( $\Delta$ ) *i*-PP/WF 3%; ( $\square$ ) *i*-PP/WF 10%; ( $\nabla$ ) *i*-PP/WF 20%.

behavior is followed by *i*-PP/WF composite melts. Figure 1 shows representative plots of shear stress–shear rate data at a given temperature 483 K.

The values of power law flow indices  $n$  of the power law relation<sup>26</sup>

$$\tau_w = K \gamma_w^n \tag{5}$$

obtained from the slopes of the plots of  $\log \tau_w$  against  $\gamma_w$  are shown in Table I. The  $n$  values were less than unity, indicating a pseudoplastic nature of the melt composites. The value of  $n$  decreases slightly with increase in filler content at all temperatures of measurement whereas for a particular filler content the value of  $n$  increases with increase in temperature. Thus the degree of pseudoplasticity of the composite melt increases with increase in filler content and decreases with an increase in temperature.

**Melt Viscosity.** Viscosity–shear rate plots of *i*-PP/WF composites are shown in Figures 2 and 3. Melt viscosities of these low modulus and porous

TABLE I  
Values of Power Law Exponent ( $n$ ) and Activation Energy for Viscous Flow ( $\Delta E$ )  
for PP/WF Composites

Sample	$n$			$\Delta E$ (kcal/mol)
	At 483 K	At 503 K	At 523 K	
PP	0.39	0.44	0.48	5.02
PP/WF (3%)	0.37	0.41	0.46	5.76
PP/WF (10%)	0.34	0.39	0.41	6.55
PP/WF (20%)	0.33	0.38	0.38	6.38

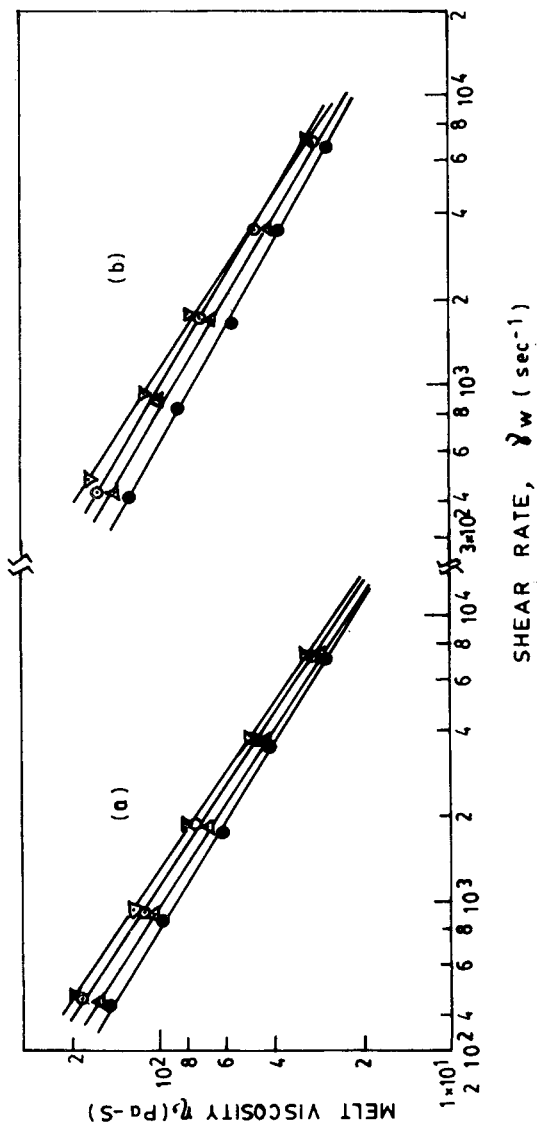


Fig. 2. Variation of melt viscosity ( $\eta$ ) with shear rate ( $\dot{\gamma}_w$ ) for i-PP (○), i-PP/WF 3% (⊙), i-PP/WF 10% (○), i-PP/WF 20% (▽), at 483 K (a) and 503 K (b).

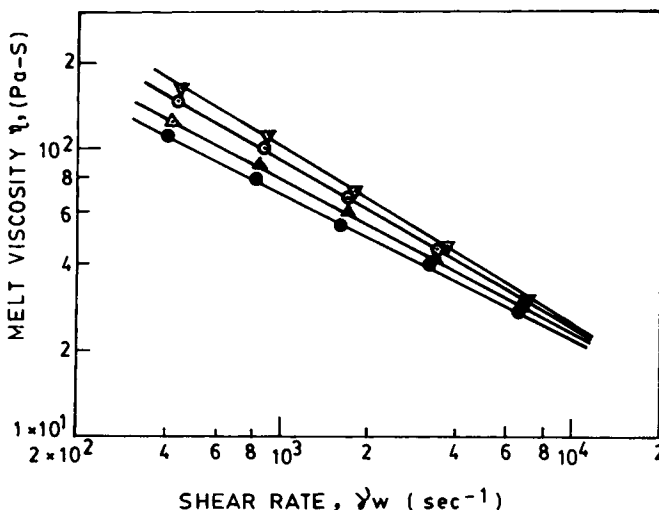


Fig. 3. Variation of melt viscosity ( $\eta$ ) with shear rate ( $\gamma_w$ ) at 523 K for: ( $\odot$ ) *i*-PP; ( $\Delta$ ) *i*-PP/WF 3%; ( $\square$ ) *i*-PP/WF 10%; ( $\nabla$ ) *i*-PP/WF 20%.

WF-filled *i*-PP composites were lower by about 1 order than the values with hard and smooth filler-containing *i*-PP composites studied by other authors.<sup>27,28</sup> It may be noted from Figures 2 and 3 that the viscosity decreases with increasing shear rate and at any given shear rate the viscosity increases with increase in filler content. However, the  $\eta$ - $\gamma_w$  plots tend to converge at very higher shear rate values and above  $\gamma_w = 10^4 \text{ s}^{-1}$  the presence of WF has little effect on shear viscosity. This tendency of  $\eta$  vs.  $\gamma_w$  plots is exhibited at all temperatures of study.

Figure 4 presents melt viscosity-shear stress plots of *i*-PP/WF composites at the three temperatures of measurements. At any given temperature the melt viscosity shows a linear decrease with increasing shear stress. Slopes of these curves are in good agreement with the power law relation<sup>26</sup> for the pseudoplastic fluids obeying eq. (5),

$$\eta = K^{1/n}(\tau_w)^{(n-1)/n} \tag{6}$$

and the values  $n$  were quite consistent with those shown in Table I.

Filled polymer melts are reported<sup>29-33</sup> to exhibit yield stress due to the formation of interparticle network which becomes quite strong at high filler loadings. Yield stress is most pronounced at low shear rates, e.g.,  $10^{-2}$  to  $10^0 \text{ s}^{-1}$ , and with very fine particle fillers. The finer the filler, the larger the ability of network formation and the stronger the network exhibiting higher yield values. All systems<sup>30</sup> exhibiting yield stress have filler diameters below  $0.5 \mu\text{m}$ . In the present work we have not observed any yield value due probably to relatively higher shear rates of study (viz.  $400$ - $7500 \text{ s}^{-1}$ ) and much larger size of the WF particles ( $200$ - $300 \mu\text{m}$ ). The absence of yield values was also reported with large particles of glass spheres<sup>34</sup> and glass as well as cellulose fibers.<sup>35,36</sup>

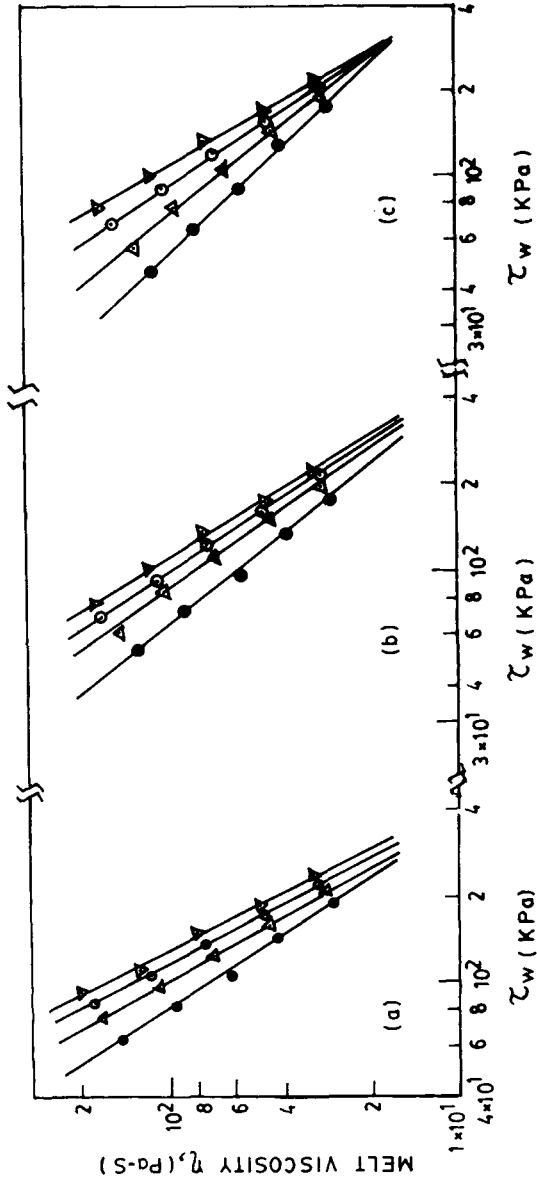


Fig. 4. Plot of melt viscosity ( $\eta$ ) with shear stress ( $\tau_w$ ) for i-PP ( $\infty$ ), i-PP/WF 3% ( $\Delta$ ), i-PP/WF 10% ( $\circ$ ), i-PP/WF 20% ( $\nabla$ ) at 483 K (a), 503 K (b), and 523 K (c).

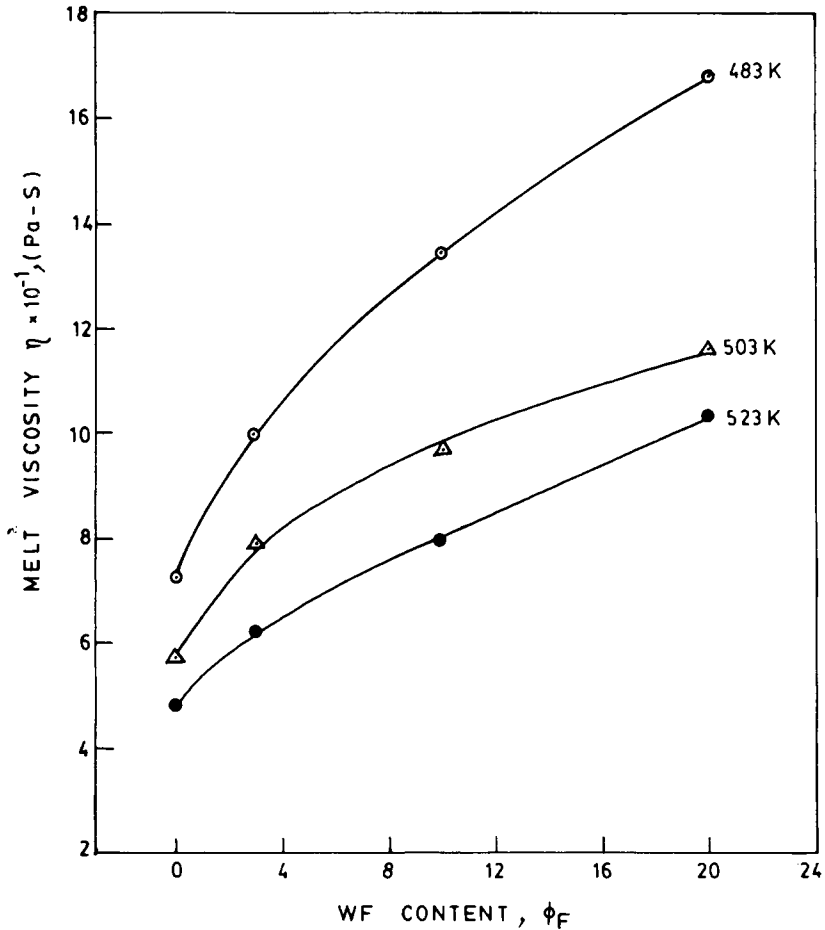
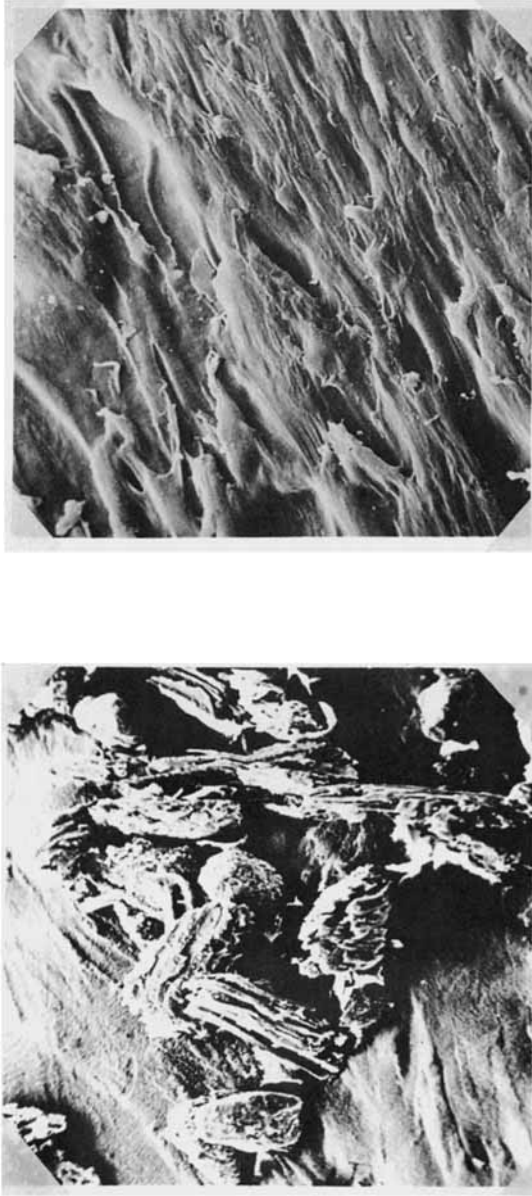


Fig. 5. Melt viscosity data of *i*-PP/WF composites at 483 K ( $\odot$ ), 503 K ( $\Delta$ ), and 523 K ( $\circ$ ) as a function of  $\phi_F$ .

Figure 5 presents the variation of melt viscosity of the composites with filler weight percent ( $\phi_F$ ) at 483 K, 503 and 523 K and at a fixed shear stress 100 kPa. Melt viscosity increases by 100–140% compared with nonfilled *i*-PP as WF concentration is increased from 0–20%, depending on the temperature. SEM photomicrographs of WF particles and impact-broken surfaces of *i*-PP/WF composites are shown in Figures 6(a–d). It may be noted that WF particles are porous and are of very irregular shape. Incorporation of WF introduces discontinuity in the *i*-PP matrix and the extent of discontinuity increases with increase in WF content in the composites. It can thus be argued that melt viscosity of *i*-PP increases due to increased obstruction produced to flow by these irregular-shaped WF particles.

#### Effect of Temperature

The viscosity decreases in a polymer melt with increase in temperature since molecular motion is facilitated at higher temperatures due to availabil-



(a)

(b)

Fig. 6. SEM photomicrographs for (a) WF particles of size 200–300  $\mu\text{m}$  ( $\times 80$ ), and impact-broken surfaces of *i*-PP/WF composites with WF content (b) 0% ( $\times 470$ ), (c) 10% ( $\times 415$ ), and (d) 20% ( $\times 415$ ).





(d)



(c)

Fig. 6. (Continued from the previous page.)

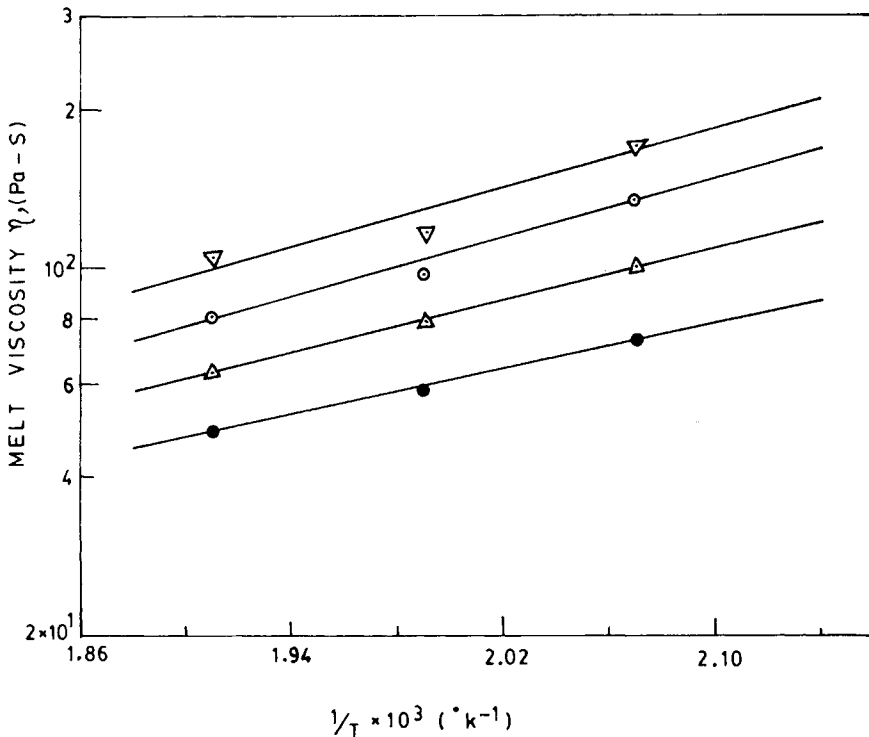


Fig. 7. Arrhenius plots of the melt viscosity data  $\log \eta$  vs.  $1/T$  for *i*-PP/WF composites at a constant shear stress 100 kPa: ( $\bullet$ ) *i*-PP; ( $\Delta$ ) *i*-PP/WF 3%; ( $\circ$ ) *i*-PP/WF 10%; ( $\nabla$ ) *i*-PP/WF 20%.

ity of greater free volume. Filled polymer melt viscosity would thus be less temperature-sensitive than the unfilled melt viscosity because only the polymer fraction in the composite contributes towards free volume change. Dependence of melt viscosity on temperature is shown in Figure 7 as the semilogarithmic Arrhenius plots  $\eta$  vs.  $1/T$  at a fixed shear stress 100 kPa. In the Arrhenius expression  $\eta$  is related to absolute temperature ( $T$ ) by the following equation<sup>37</sup>:

$$\eta = A \exp(\Delta E/RT) \quad (7)$$

where  $A$  is a constant characteristic of the polymer,  $\Delta E$  is the activation energy for viscous flow, and  $R$  is the universal gas constant. From the slopes of these plots  $\Delta E$  values were estimated and are presented in Table I. It may be noted that  $\Delta E$  of the composite melt increases inappreciably with increase in the WF concentration, indicating that melt viscosity of the composites is less temperature-sensitive than that of the nonfilled polymer. Such an observation is in good agreement with other published results.<sup>27, 38, 39</sup>

### Melt Elasticity

The melt elasticity parameters such as die swell ratio, first normal stress difference, recoverable shear strain, and the apparent shear modulus of *i*-PP/WF composites were evaluated at a temperature of 483 K. The die swell

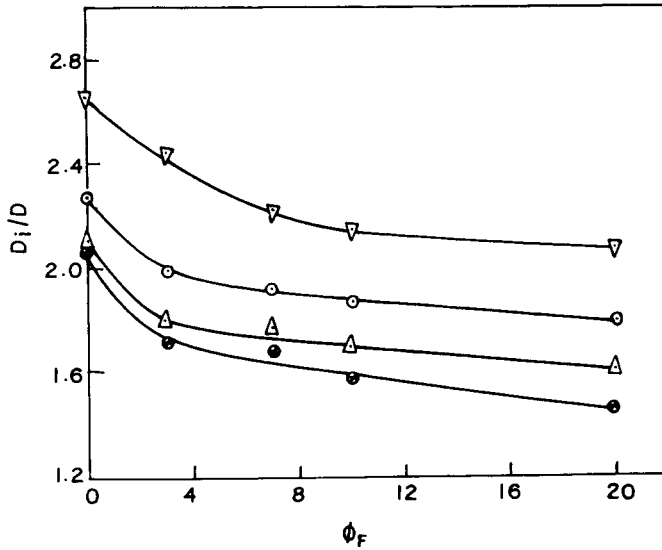


Fig. 8. Variation of die swell ratio ( $D_i/D$ ) with WF content at constant shear stress (kPa): ( $\otimes$ ) 92; ( $\Delta$ ) 105; ( $\circ$ ) 140; ( $\nabla$ ) 190.

ratio is given by  $D_i/D$ , where  $D_i$  and  $D$  are the diameters of the extrudate and the die, respectively. The first normal stress difference ( $\tau_{11} - \tau_{22}$ ) was determined using Tanner's equation<sup>40</sup>:

$$\tau_{11} - \tau_{22} = 2\tau_w [2(D_i/D)^6 - 2]^{1/2} \tag{8}$$

Recoverable shear strain ( $\gamma_R$ ) and apparent shear modulus ( $G$ ) were estimated from the following expressions used also by other authors<sup>26,41</sup>:

$$\gamma_R = (\tau_{11} - \tau_{22})/2\tau_w \tag{9}$$

$$G = \tau_w/\gamma_R \tag{10}$$

First normal stress difference values for *i*-PP/WF composites were about 1–2 orders higher than the values reported by Han and co-workers<sup>27,28</sup> for hard inorganic and smooth filler containing *i*-PP composites. Variation of die swell ratio and first normal stress difference are presented in Figures 8 and 9, respectively, as function of  $\phi_F$  at various fixed shear stress values and at 483 K. These melt elasticity parameters were found to decrease with increase in WF content. At any given shear stress the decrease in elasticity with increase in WF content was marginal in the regions beyond  $\phi_F = 3$ . The total drop in die swell ratio and in first normal stress difference were 8–15% and 5–25%, respectively, based on the value of nonfilled *i*-PP, depending on the shear stress. It has been shown in the previous section (Fig. 6) that the presence of WF creates discontinuity in the polymer matrix. Melt elasticity decrease in these composites may be attributed to this phenomena, which in consequence would cause discontinuity in stress transfer for elastic recovery or deformation. Furthermore, WF particles are soft and porous and may undergo distor-

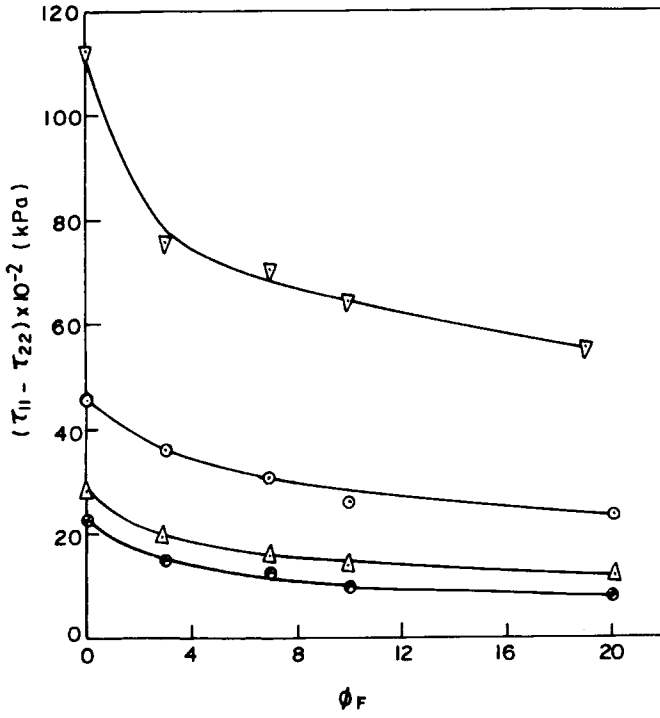


Fig. 9. Plots of first normal stress difference ( $\tau_{11} - \tau_{22}$ ) vs. WF content ( $\phi_F = \text{wt}\%$ ) at constant shear stress (kPa); ( $\otimes$ ) 92; ( $\Delta$ ) 105; ( $\circ$ ) 140; ( $\nabla$ ) 190.

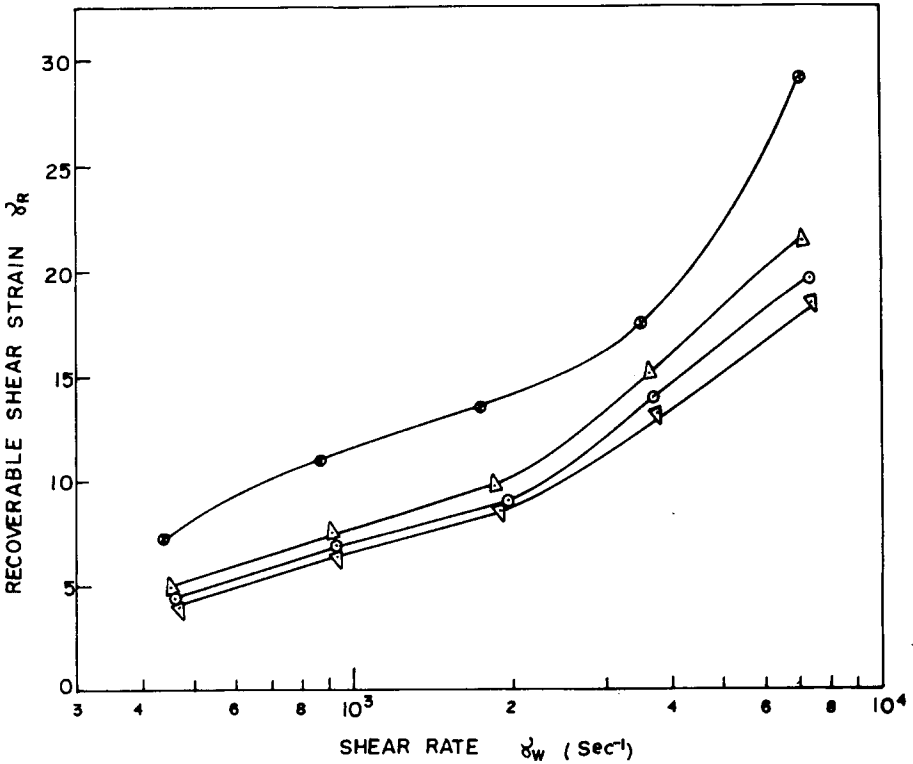


Fig. 10. Recoverable shear strain ( $\gamma_R$ ) vs. shear rate ( $\gamma_w$ ) plots at constant WF concentration: ( $\otimes$ ) 0; ( $\Delta$ ) 3%; ( $\circ$ ) 10%; ( $\nabla$ ) 20%.

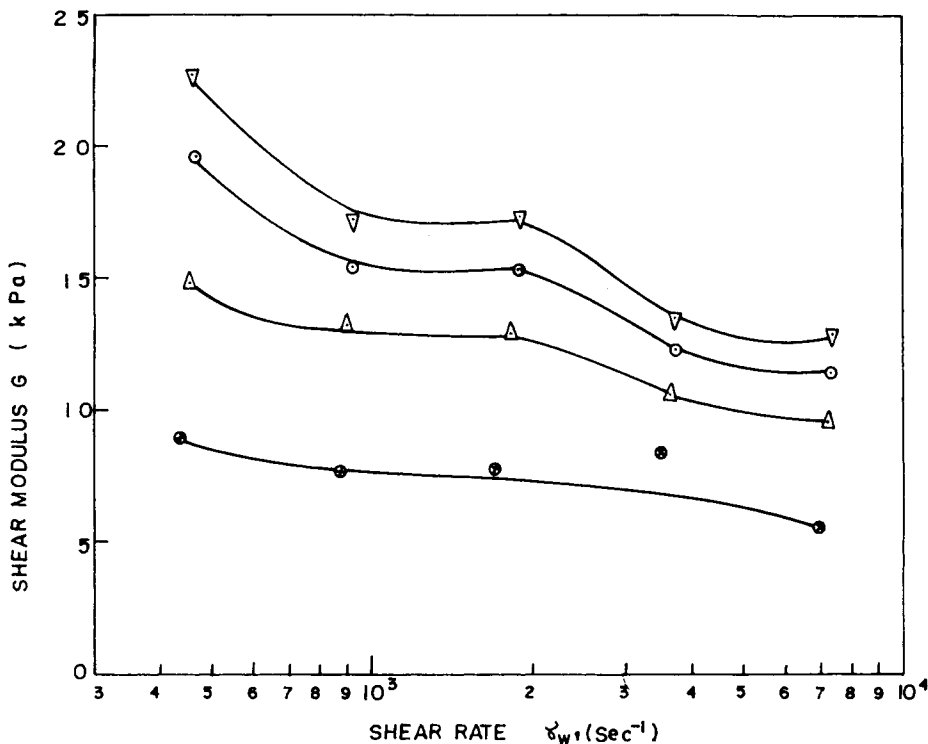


Fig. 11. Variation of apparent shear modulus ( $G$ ) with shear rate ( $\dot{\gamma}_w$ ) at constant WF concentration: ( $\otimes$ ) 0%; ( $\Delta$ ) 3%; ( $\circ$ ) 10%; ( $\nabla$ ) 20%.

tion, absorbing in the process some energy from the elastic deformation or recovery stresses. This observation of melt elasticity decrease in filled polymer composites is in good agreement with other published results.<sup>27,28,30</sup> Decrease in these melt elasticity parameters of *i*-PP in the presence of WF filler aids in processing safety by increasing the critical shear stress for melt fracture. This will give smooth surface of the extrudates of the composites. Recoverable shear strain  $\gamma_R$  increases, and apparent shear modulus  $G$  decreases with increasing shear rate at a fixed temperature of 483 K (Figs. 10 and 11). At any fixed shear rate  $\gamma_R$  decreases and  $G$  increases with increasing WF concentration.

### CONCLUSIONS

*i*-PP/WF composites obeyed the power law relationship between shear stress and shear rate over the entire studied range of shear rates (viz. from 400 to 7500  $\text{s}^{-1}$ ) and at all WF concentrations, with the power law exponent varying from 0.3 to 0.5. This suggests a pseudoplastic nature of the melt of these composites. At any given temperature the value of the power law index decreases with increasing WF content. Melt viscosity decreases with increasing shear rate and increases with increasing WF concentration at any given temperature. Melt elasticity parameters such as die swell ratio, first normal

stress difference, and shear modulus decrease while recoverable shear strain increases with increasing WF content in the composites.

### References

1. J. A. Brydson, *Plastics Materials*, 3rd ed., Newnes-Butterworths, London, 1975, Chap. 11.
2. D. R. Paul and S. Newman, *Polymer Blends*, Academic, New York, 1978, Vol. 2.
3. F. C. Stehling, T. Huff, C. S. Speed, and G. Wissler, *J. Appl. Polym. Sci.*, **26**, 2693 (1981).
4. G. G. A. Bohn, G. R. Hamed, and L. E. Yescilius, Ger. Offen. 2,825,697 (1978).
5. C. Markin and H. L. William, *J. Appl. Polym. Sci.*, **25**, 2451 (1980).
6. A. K. Gupta and S. N. Purwar, *J. Appl. Polym. Sci.*, **29**, 1595 (1984).
7. A. Yamaguchi, *Plastic Age*, **B**, 41(4), 6 (1967).
8. P. Harrison and R. F. Shippard, *Plast. Polym.*, **39**(140), 103 (1971).
9. J. H. Peltz (Jr.), Ger. Offen. 2,005,797 (1970).
10. J. Rusznack et al., *Muanyg Gummi*, **16**(9), 257 (1970).
11. H. G. Trieschmann et al., Ger. Offen. 2,033,803 (1972).
12. T. Nakanishi and M. Morita, *Chem. Abstr.*, **85**, 193625u (1976).
13. S. J. Monte and G. Sugerman, *Ken-React Reference Manual—Titanate and Zirconate Coupling Agents*, Bulletin No. KR-1084L, Kenrich Petrochemicals, Inc., N.J., 1985.
14. P. D. Richtie, Ed., *Plasticisers, Stabilisers and Fillers*, Iliffe, London, 1972, Part 3.
15. H. Ohkawa, S. Tamura, N. Sasaki, and H. Kaji, *Chem. Abstr.*, 86,172521n (1977).
16. H. Matsukawa, A. Yoshijima, and H. Yokoyama, *Chem. Abstr.*, 85,6675a (1976).
17. S. Ishihara, H. Sasaki, I. Osada, J. Hasegawa, and H. Kajiwara, *Mokuzai Kogyo*, **35**(395), 71 (1980).
18. G. R. Lightsey, H. Paul, K. S. Kalasinsky, and L. Mann, *J. Miss. Acad. Sci.*, **24**, 76 (1979).
19. S. N. Maiti and K. Singh, *J. Appl. Polym. Sci.*, **32**, 4285 (1986).
20. I. A. Gamova, T. V. Makhova, V. B. Vikhрева, A. V. Bryskovskaya, V. V. Mikhailova, and E. V. Umanskaya, *Izv. Vyssh. Uchebn. Zaved., Lesn. Zh.*, **2**, 80 (1979).
21. I. Dentshev, L. Bosreliev, and M. Athanasova, *Plasteu Kautsch*, **29**(9), 537 (1982).
22. H. Ikeda, *Chem. Abstr.*, **85**, 193615r (1976).
23. Operation, Maintenance and Installation Instructions, MCR Capillary Rheometer, Catalog No. 3210-001, Manual No. 10-49-1(c), p. 11.
24. J. A. Brydson, *Flow Properties of Polymer Melts*, Iliffe, London, 1970.
25. S. Middleman, *The Flow of High Polymers*, Wiley-Interscience, New York, 1968.
26. C. D. Han, *Rheology in Polymer Processing*, Academic, New York, 1976.
27. C. D. Han, *J. Appl. Polym. Sci.*, **18**, 821 (1974).
28. C. D. Han, T. Van Den Weghe, P. Shete, and J. R. Haw, *Polym. Eng. Sci.*, **21**, 196 (1981).
29. H. Tanaka and J. L. White, *Polym. Eng. Sci.*, 20,949 (1980).
30. Y. Suetsugu and J. L. White, *J. Appl. Polym. Sci.*, **28**, 1481 (1983).
31. D. M. Bigg, *Polym. Eng. Sci.*, **23**, 206 (1983).
32. F. M. Chapman and T. S. Lee., *Soc. Plast. Eng. J.*, **26**(1), 37 (1970).
33. T. Kataoka, T. Kitano, M. Sasahara, and K. Nishijima, *Rheol. Acta*, **17**, 149 (1978).
34. J. L. White, L. Czarnecki, and H. Tanaka, *Rubber Chem. Technol.*, **53**, 823 (1980).
35. Y. Chan, J. L. White, and Y. Oyanagi, *Trans. Soc. Rheol.*, **22**, 507 (1978).
36. L. Czarnecki and J. L. White, *J. Appl. Polym. Sci.*, **25**, 1217 (1980).
37. J. M. McKelvey, *Polymer Processing*, Wiley, New York, 1962.
38. D. R. Saini, A. V. Shenoy, and V. M. Nadkarni, *Polym. Comp.*, **7**, 193 (1986).
39. S. N. Maiti and P. K. Mahapatro, *J. Polym. Mater.*, to appear.
40. R. I. Tanner, *J. Polym. Sci.*, A-2, **8**, 2067 (1970).
41. A. F. Plochocki, in *Polymer Blends*, D. R. Paul and S. Newman, Eds., Academic, New York, 1978, Vol. 2.

Received April 26, 1988

Accepted May 2, 1988